Bioorganic & Medicinal Chemistry Letters 21 (2011) 6773–6777

Contents lists available at SciVerse ScienceDirect

Bioorganic & Medicinal Chemistry Letters

journal homepage: www.elsevier.com/locate/bmcl

Discovery of a new class of glucosylceramide synthase inhibitors

Elena Koltun, Steven Richards *, Vicky Chan, Jason Nachtigall, Hongwang Du, Kevin Noson, Adam Galan, Naing Aay, Art Hanel, Amanda Harrison, Jeff Zhang, Kwang-Ai Won, Danny Tam, Fawn Qian, Tao Wang, Patricia Finn, Kathleen Ogilvie, Jon Rosen, Raju Mohan, Christopher Larson, Peter Lamb, John Nuss, Patrick Kearney

Exelixis, 210 E. Grand Avenue, South San Francisco, CA 94005, USA

ARTICLE INFO

Article history:
Received 25 August 2011
Revised 8 September 2011
Accepted 12 September 2011
Available online 17 September 2011

Keywords:
Glucosylceramide synthase inhibitor
GCS
Diabetes
Gaucher disease
Cancer
Inflammation

ABSTRACT

A novel series of potent inhibitors of glucosylceramide synthase are described. The optimization of biochemical and cellular potency as well as ADME properties led to compound **23c**. Broad tissue distribution was obtained following oral administration to mice. Thus **23c** could be another useful tool compound for studying the effects of GCS inhibition in vitro and in vivo.

Glucosylceramide synthase (GCS) is a glucosyltranserase that processes the sphingolipid ceramide (**1**) (Fig. 1). The product, glucosylceramide (**2**), can be further elaborated with a variety of oligosaccharides to become glycosphingolipids called gangliosides (most notably GM1 and GM3 (**3**)). Excess glycosphingolipids have been correlated with a variety of human diseases.[1] The pathologies associated with lysosomal storage disorders (Gaucher, Fabry, Tay-Sachs, and Sandhoff) stem from improper disposal of glucosylceramide and other glycosphingolipids.[2] Excess ganglioside GM3 has been linked to insulin resistance wherein GM3 in the cell membrane forms lipid rafts that disrupt the membrane environment around the insulin receptor. As a result of this perturbation, the insulin receptor does not signal properly resulting in insulin resistance.[3] In addition, disregulated glycosphingolipids have been implicated in multi-drug resistance, atherosclerosis and inflammation.[4–6]

The beneficial effects of small molecule inhibition of GCS have been well studied. There are two "privileged" classes from which most known GCS inhibitors arise (Fig. 2). The iminosugar class is well represented by Migustat (**4**) (Zavesca®) and AMP-DNM (**5**).[7,8] These compounds are also potent inhibitors of intestinal glycosidases.[9] Miglustat (**4**) is available as substrate reduction therapy (SRT) for patients who are not candidates for enzyme replacement therapy (ERT). It is also used to treat Niemann-Pick type C disease and has shown efficacy in patients with cystic fibrosis.[10] A large scale synthesis of AMP-DNM (**5**) was recently reported to support pre-clinical development.[11]

Ceramide analogs are best represented by Genz-123346 (**6**) and Genz-112638 (**7**).[12–14] Genz-123346 (**6**) has been used to prove the concept that chronic GCS inhibition can ameliorate insulin resistance in animal models of diabetes.[12] Genz-112638 (**7**) has advanced to phase 3 clinical trials as SRT for type 1 Gaucher disease.

Given the broad therapeutic potential of small molecule GCS inhibitors, we sought to determine if other compound classes could modulate GCS activity. As GCS is expressed throughout the body, the goal was to identify potent inhibitors with systemic exposure and minimal off-target effects.

To that end, we embarked on an HTS campaign in which our library of over 4 million compounds was tested in a coupled assay format. GCS activity was measured as the amount of UDP-glucose consumed during the synthase-catalyzed reaction (Fig. 3). Upon quenching, remaining UDP-glucose was processed by UDP-glucose dehydrogenase, producing NADH. The NADH formed then participated in a diaphorase mediated reduction of resazurin (**8**) to fluorescent resorufin (**9**). This assay was sufficiently robust to also serve as the primary assay for our hit-to-lead research efforts.

The screen yielded a variety of potent hits. One of which was the racemic dipeptide shown in Figure 4. After both enantiomers were synthesized, the *R* isomer (**10**, derived from D serine) was found to be about 80 fold more potent than the *S* isomer (**11**). This

* Corresponding author. Tel.: +1 650 837 7000; fax: +1 650 837 8177.
E-mail address: srichard@exelixis.com (S. Richards).

0960-894X/$ - see front matter © 2011 Elsevier Ltd. All rights reserved.
doi:10.1016/j.bmcl.2011.09.037

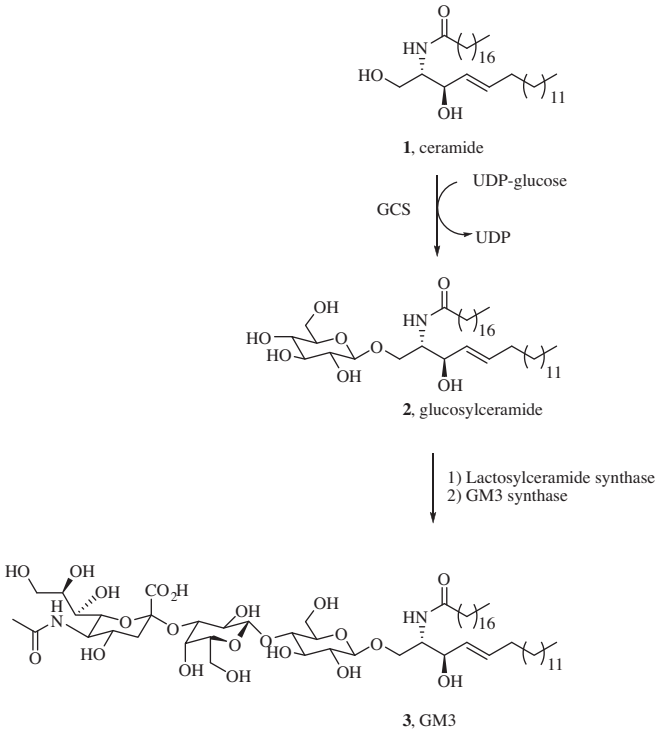

Figure 1. GCS mediated glycosphingolipid synthesis.

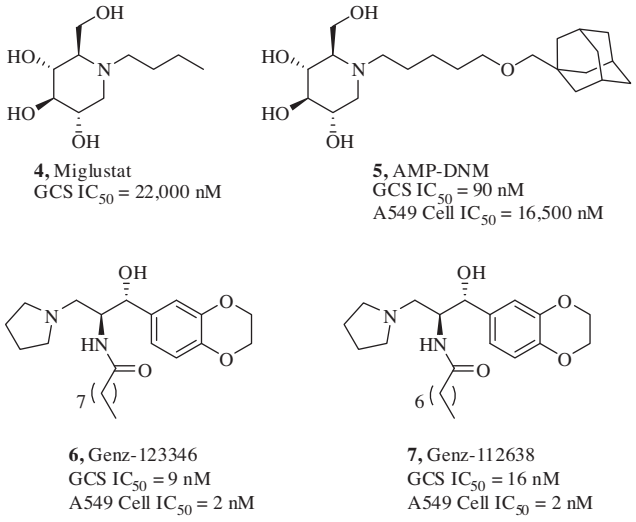

Figure 2. Representative GCS inhibitors.[22]

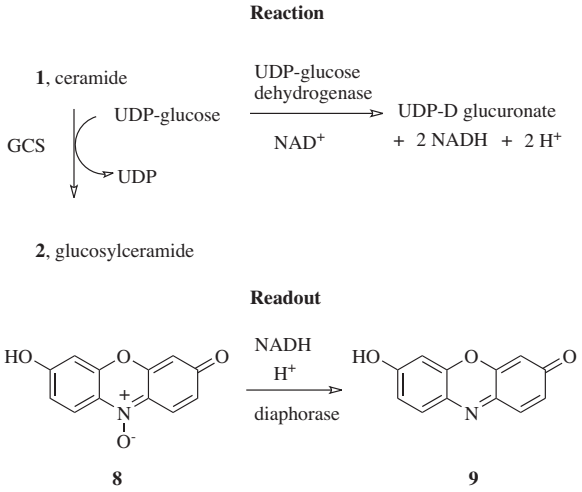

Figure 3. GCS biochemical screen.

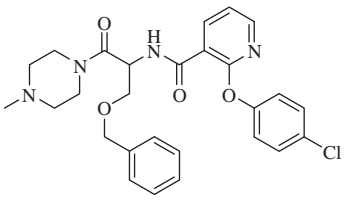

Figure 4. HTS hit.

stereochemical preference was confirmed by the preparation of analogous enantiomer pairs (data not shown). Thus we decided to begin developing SAR around active enantiomer **10**.

The synthesis of aryl ether analogs (**16**) is shown in Scheme 1. Benzyl protected, *N*-boc serine (**12**) was coupled with *N*-methyl piperazine under standard conditions. Following acid mediated boc deprotection, the resulting amine (**13**) was ready for coupling with acid **15**. The acid (**15**) was prepared in a two step procedure starting from the appropriately substituted ethyl-2-chloronicotinates (**14**). The S_NAr displacement of the chloride with substituted phenols required heating to 120 °C in a sealed tube under basic conditions. The resulting ester was hydrolyzed and the two partners (**15** and **13**) were coupled to provide the desired aryl ether analogs (**16**).

Substituted serine derivatives (**18**) were prepared as shown in Schemes 2 and 3. The dianion of boc-serine was generated using NaH in DMF and trapped with the appropriately substituted alkyl bromide (Scheme 2).[15] The resulting acid was coupled with *N*-methyl piperazine using HATU to generate boc amide **17**. Compound **17** was then deprotected under acidic conditions and coupled with acid **15** to yield serine analogs (**18**).

Boc-aziridine methyl ester **20** was prepared in three steps from boc-serine methyl ester (**19**) in an analogous manner to what has been reported (Scheme 3).[16] Activation of **19** as the mesylate followed by boc-deprotection, cyclization and re-protection proceeded smoothly. The aziridine (**20**) was then subjected to Lewis acid mediated opening with alcohols.[17] Acidic boc deprotection and HATU coupling of the resulting amine with acid **15** provided ester **21**. This ester was hydrolyzed and coupled with *N*-methyl piperazine to furnish serine analogs **18f** and **18g**.

Analogs of the western amide portion of the scaffold were synthesized as shown in Scheme 4. Boc-benzyl serine (**12**) was treated with methanolic HCl to both deprotect the boc group and form the methyl ester.[18] The resulting amino ester was coupled with the appropriately substituted acid (**15**) and hydrolyzed to form acid **22**. HATU coupling with amines followed to provide the desired analogs (**23**). In the case of compounds **23c–d**, boc amines were coupled, necessitating a subsequent acidic deprotection step.

A summary of our efforts to develop aryl ether SAR is shown in Table 1. Early work on this portion of the scaffold revealed that the aryl ether substituent appended to the pyridine was required for activity. Substitution of that aryl ring was tolerated. The para chlorophenyl substituent of lead **10** could be replaced by a methyl group (**16a**) without losing potency. However, deletion of the 4-chlorophenyl substituent resulted in analog **16b** which was 30

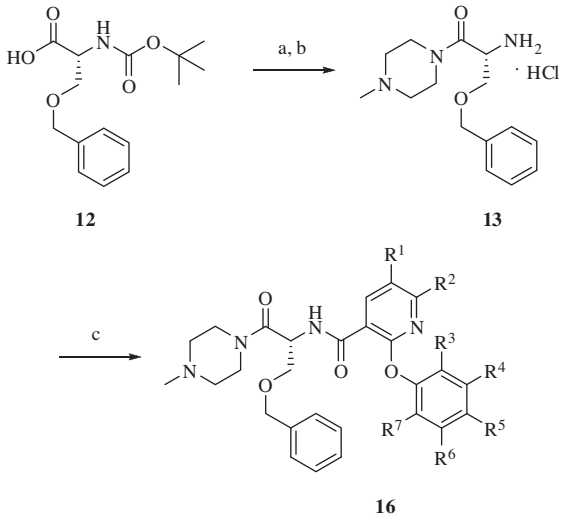

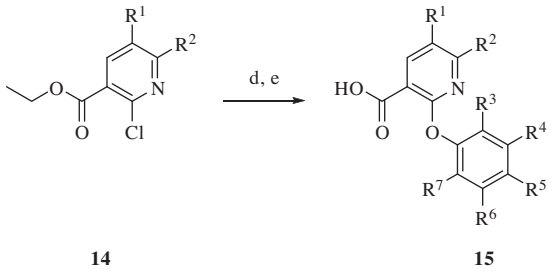

Scheme 1. Reagents and conditions: (a) EDC, HOBt, $CHCl_2$, *N*-methylpiperazine, rt, 8 h; (b) 4 M HCl in dioxane, MeOH, 55 °C, 3 h; (c) HATU, MeCN, Hünig's base, **15**, rt, 6 h; (d) Cs_2CO_3, DMA, 120 °C, 48 h; (e) LiOH, THF, H_2O, 100 °C, 4 h.

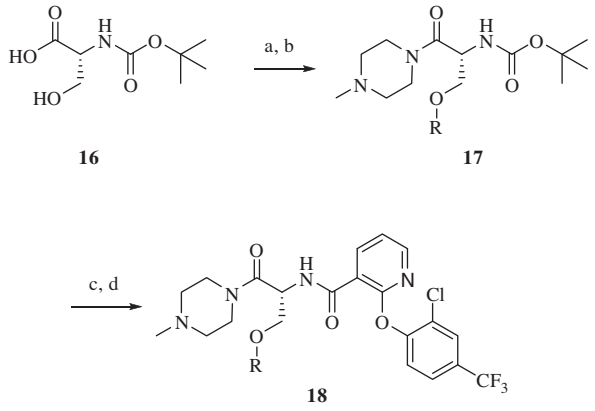

Scheme 2. Reagents and conditions: (a) NaH, DMF,0 °C, bromide, 18 h; (b) EDC, HOBt, $CHCl_2$, *N*-methylpiperazine, rt, 8 h; (c) 4 M HCl in dioxane, MeOH, 55 °C, 3 h; (d) HATU, DCE, **15**, rt, 18 h.

fold less potent. Replacing the 4-chloro substituent with a fluoro group (**16c**) also resulted in a less potent compound, losing 10 fold activity. Activity was not improved by the addition of an ortho fluoro substituent (**16d**) but this substitution pattern was tolerated. The 2,6-dichlorophenyl analog (**16e**) was also tolerated but remained 10 fold less potent than lead **10**. Meta substitution with a polar dimethyl amino group (**16f**) was not well tolerated. Similarly, 3,4-dimethyl substitution resulted in analog **16g** that was poorly active.

Modification of the pyridine ring could be accomplished without a significant negative impact on potency. For example,

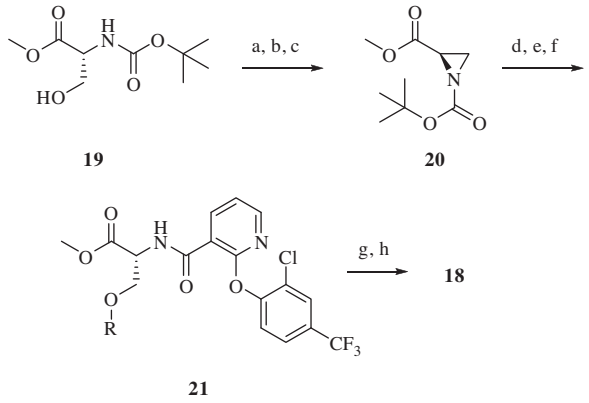

Scheme 3. Reagents and conditions: (a) MsCl, Et_3N, THF, 0 °C to rt, 18 h; (b) 4 M HCl in dioxane, Et_2O, rt, 18 h; (c) (i) Hünig's base, MeCN, 60 °C, 8 h. (ii) $(Boc)_2O$, Hünig's base, MeCN, rt, 18 h; (d) alcohol, $BF_3{\cdot}OEt_2$, $CHCl_3$, rt, 18 h; (e) 4 M HCl in dioxane, rt, 18 h; (f) HATU, DCE, **15**, rt, 18 h; (g) LiOH, THF, H_2O, rt, 1 h; (h) EDC, HOBt, $CHCl_2$, *N*-methylpiperazine, rt, 8 h.

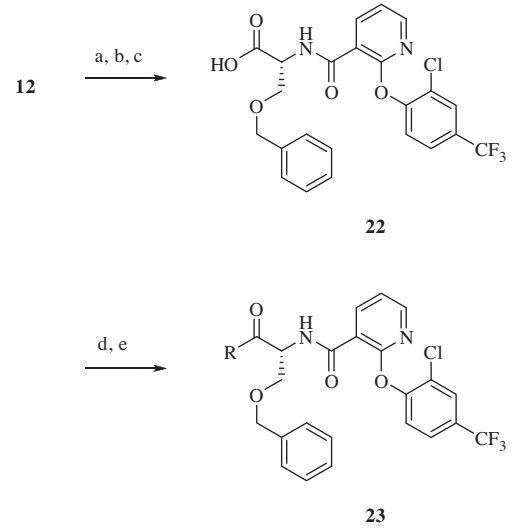

Scheme 4. Reagents and conditions: (a) TMSCl, MeOH, rt, 18 h; (b) HATU, DCE, **15**, rt, 18 h; (c) LiOH, THF, H_2O, rt, 1 h; (d) amine, HATU, DCE, rt, 18 h; (e) 4 M HCl in dioxane, MeOH, 55 °C, 3 h (only for compounds **23c–d**).

compounds **16h** and **16i** were both marginally less active than lead **10**. When the 3-fluro pyridyl substituent was combined with 2,4-dichloro phenyl ether, the resulting compound, **16j**, was 10 fold more potent that lead **10**. This increased potency was found to be driven entirely by the aryl ether substitution, as evidenced by the 2,4-dichlorophenyl analog **16k**. The 2-methyl, 4-chloro phenyl analog **16m** was similarly potent. Analog **16n** with its 2-Chloro, 4-triflurometyl phenyl substitution was 30 fold more potent than lead compound **10**. Thus the 2,4-disubstitued aryl ether motif was shown to provide the most significant potency improvement and was conserved for subsequent SAR development.

With the optimal aryl ether substitution established, the scope of serine substitution was explored (Table 2). To better differentiate this set of compounds, cellular potency and certain ADME characteristics were determined. The cellular readout used was the quantitation of ganglioside GM1 on the surface of A549 cells.[19] Decreased glucosylceramide synthesis would lead to decreased GM1 synthesis. CYP3A4 inhibition was also measured by incubating compounds with human liver microsomes and observing their ability to impede oxidative metabolism of testosterone.[20] Incubation with mouse liver microsomes was performed to gauge compound susceptibility to oxidative degradation.[21]

Table 1
Aryl ether analogs (**16**)

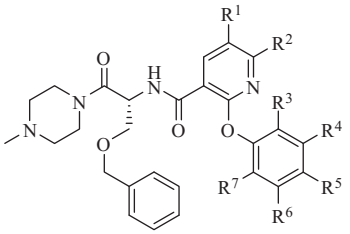

Compound	R_1	R_2	R_3	R_4	R_5	R_6	R_7	GCS IC_{50}[a] (nM)
10	H	H	H	H	Cl	H	H	32
16a	H	H	H	H	Me	H	H	53
16b	H	H	H	H	H	H	H	1,150
16c	H	H	H	H	F	H	H	300
16d	H	H	F	H	F	H	H	230
16e	H	H	Cl	H	H	H	Cl	340
16f	H	H	H	NMe_2	H	H	H	1,075
16g	H	H	H	Me	Me	H	H	1,080
16h	H	Me	H	H	Cl	H	H	90
16i	Br	H	H	H	Cl	H	H	110
16j	F	H	H	H	Cl	H	H	180
16k	F	H	Cl	H	Cl	H	H	3
16l	H	H	Cl	H	Cl	H	H	2
16m	H	H	Me	H	Cl	H	H	2
16n	H	H	Cl	H	CF_3	H	H	1

[a] Average value of duplicate experiments reported.

Benzyl serine **16n** was found to be as potent in cells as it was biochemically. It had a minimal CYP3A4 liability and was modestly stable. Dihydrobenzodioxine analog **18a** maintained biochemical and cellular potency relative to **16n** but was less stable to microsomal oxidation. Compound **18a** was also a more potent CYP3A4 inhibitor. 4-Fluorobenzyl analog **18b** was about half a log less potent than **16n** and had a less desirable ADME profile.

In an effort to find benzyl group replacements, heterocycles were investigated. This is because earlier work in this area established the fact that the serine had to be alkylated in order to maintain activity. While the 2-methyl oxazole derivative (**18c**) was tolerated, it was significantly less potent than **16n**. It had no measurable CYP3A4 liability but was only modestly stable in mouse microsomes. 4-pyridyl derivative **18d** was almost 300 fold less potent than **16n** with a significant CYP3A4 liability and comparable metabolic stability. Interestingly, the addition of a 3-chloro group (**18e**) significantly improved potency and decreased the CYP3A4 liability without increasing metabolic stability. Of the aliphatic serine analogs prepared, *tert*-butyl ether **18f** was also significantly less potent than lead **16n** with a similar ADME profile. Cyclopropylmethyl ether **18g** was not a considerable improvement over **18f**. Thus it was determined that the unsubstituted benzyl serine moiety provided the best balance of GCS inhibitory potency and desirable ADME properties.

The final focus of SAR development on this scaffold was the western amide portion. A summary of this work is shown in Table 3. There was very little flexibility in this portion of the scaffold. Non basic amides were generally not tolerated (data not shown). Many active amides which did contain a basic amine had undesirable ADME profiles. Compounds **23a** and **23b** are examples of this phenomenon. While the amino pyrrolidide **23b** was 3 fold more potent than amino azetidide **23a**, both were metabolically unstable. We speculated that the low metabolic stability of these compounds was due to N-dealkylation. Screening of the mono *N*-methyl amino pyrrolidide diastereomers, **23c** and **23d**, supported our hypothesis in that both were significantly more metabolically stable. Fortunately, **23c** also had excellent cell potency and only a modest CYP3A4 liability. Further efforts to identify basic amides which might be metabolically stable led us to amino-quinuclidide diastereomers **23e** and **23f**. Both of these compounds were potent biochemically and in cells, inactive against CYP3A4 and had modest metabolic stability. The identification of compound **23c** demonstrated that it was possible to achieve a desirable compound profile by tuning the western amide portion of the scaffold.

Table 2
Serine analogs (**18**)

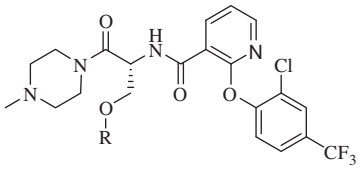

Compound	R	GCS IC_{50}[a] (nM)	A549 Cell IC_{50}[b,c] (nM)	CYP3A4 IC_{50} (nM)	Mouse liver microsome stability (% conversion)
16n		1	2	13,500	50
18a	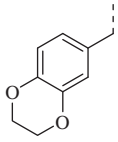	1	0.3	3,300	85
18b	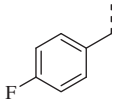	7	13	6,300	75
18c	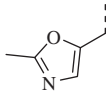	20	50	>20,000	60
18d		275	na	2,000	60
18e	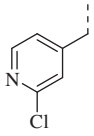	50	na	11,000	75
18f		120	na	12,000	50
18g		50	na	>20,000	50

[a] Average value of duplicate experiments reported.
[b] Average value of triplicate experiments reported.
[c] Na = data not available.

During the course of this work, **23c** emerged as a compound that combined potent in vitro GCS inhibition with acceptable ADME parameters. When **23c** was dosed in mice, significant levels of the compound were measured in plasma, liver, fat and muscle 4 h post a 30 mg/kg oral dose (Table 4).

In summary, HTS efforts identified a unique GCS inhibitor (**10**). That hit was elaborated into lead **23c** which had improved cellular potency and ADME properties. Furthermore, **23**c has a comparable biochemical profile to Genz-112638. The distribution to metabolically active tissues, especially liver, was desirable given our interest in diabetes therapy. As such, **23c** represents a novel GCS inhibitor that might be an additional valuable tool for measuring the effects of GCS inhibition in vitro and in vivo.

Table 3
Amide analogs (**23**)

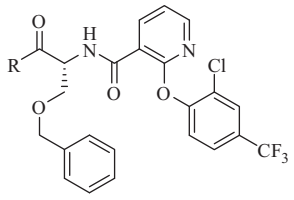

Compound	R	GCS IC_{50}[a] (nM)	A549 Cell IC_{50}[b,c] (nM)	CYP3A4 IC_{50} (nM)	Mouse liver microsome stability (% conversion)
23a	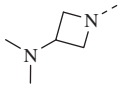	40	na	5,400	90
23b	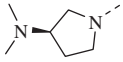	10	na	7,200	90
23c	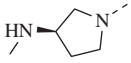	16	5	12,000	20
23d	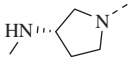	65	na	9,000	40
23e	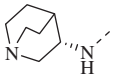	5	4	>20,000	40
23f	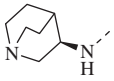	7	12	>20,000	50

[a] Average value of duplicate experiments reported.
[b] Average value of triplicate experiments reported.
[c] Na = data not available

Table 4
Mouse tissue exposure for **23c**

Compound	Plasma[a] (μM)	Muscle (μM)	Fat (μM)	Liver (μM)
23c	2	7	2	20

[a] C57BL6 mouse (n = 3), 30 mpk, PO, data collected 4 h post dose.

Acknowledgments

The authors are grateful to Sean Wu, Lory Tan, and John Bui for collecting the reported ADME data. We would also like to thank Ron Aoyama, Michael Yakes, Les Bornheim and Artur Plonowski for obtaining the mouse PK data. Finally, we would like to acknowledge our colleagues in the compound repository, Eliana Bustamante, Dorothy Trent, Melanie Dimapasoc, Yelena Zherebina, Shaun Nguyen, and Josh Rulloda, for their support of this project.

References and notes

1. For an excellent recent review of glycosphingolipid biology, see: Wennekes, T.; van den Berg, R.; Boot, R.; van der Marel, G.; Overkleeft, H.; Aerts, J. *Angew. Chem., Int. Ed.* **2009**, *48*, 8848.
2. Butters, T.; Mellor, H.; Narita, K.; Dwek, R.; Platt, F. *Phil. Trans. R. Soc. Lond. B* **2003**, *358*, 927.
3. Tagami, S.; Inokuchi, J.; Kabayama, K.; Yoshimura, H.; Kitamura, F.; Uemura, S.; Ogawa, C.; Ishii, A.; Saito, M.; Ohtsuka, Y.; Sakaue, S.; Igarashi, Y. *J. Biol. Chem.* **2002**, *277*, 3085.
4. (a) Bleicher, R.; Cabot, M. *Biochim. Biophys. Acta* **2002**, *1585*, 172; (b) Kok, J.; Sietsma, H. *Curr. Drug Targets* **2004**, *5*, 375.
5. Summers, S. *Prog. Lipid Res.* **2006**, *45*, 42.
6. Karman, J.; Tedstone, J.; Gumlaw, N.; Zhu, Y.; Yew, N.; Siegel, C.; Guo, S.; Siwkowski, A.; Ruzek, M.; Jiang, C.; Cheng, S. *Int. Immunol.* **2010**, *22*, 593.
7. Giraldo, P.; Alfonso, P.; Atutxa, K.; Fernández-Galán, M.; Barez, A.; Franco, R.; Alonso, D.; Martin, A.; Latre, P.; Pocovi, M. *Haematologica* **2009**, *94*, 1771.
8. Aerts, J.; Ottenhoff, R.; Powlson, A.; Grefhorst, A.; van Eijk, M.; Dubbelhuis, P.; Aten, J.; Kuipers, F.; Serlie, M.; Wennekes, T.; Sethi, J.; O'Rahilly, S.; Overkleeft, H. *Diabetes* **2007**, *56*, 1341.
9. Wennekes, T.; Meijer, A.; Groen, A.; Boot, R.; Groener, J.; van Eijk, M.; Ottenhoff, R.; Bijl, N.; Ghauharali, K.; Song, H.; O'Shea, T.; Liu, H.; Yew, N.; Copeland, D.; van den Berg, R.; van der Marel, G.; Overkleeft, H.; Aerts, J. *J. Med. Chem.* **2010**, *53*, 689.
10. Actelion Smadar trial registry. http://trials.actelion.com/asp/Trial_Registry/ListStudy.asp?PN=ACT-149071 (accessed September 2011).
11. Wennekes, T.; Lang, B.; Leeman, M.; van der Marel, G.; Smits, E.; Weber, M.; van Wiltenburg, J.; Wolberg, M.; Aerts, J.; Overkleeft, H. *Org. Process Res. Dev.* **2008**, *12*, 414.
12. Zhao, H.; Przybylska, M.; Wu, I.; Zhang, J.; Siegel, C.; Komarnitsky, S.; Yew, N.; Cheng, S. *Diabetes* **2007**, *56*, 1210.
13. Peterschmitt, M.; Burke, A.; Blankstein, L.; Smith, S.; Puga, A.; Kramer, W.; Harris, J.; Mathews, D.; Bonate, P. *J. Clin. Pharmacol.* **2011**, *51*, 695.
14. McEachern, K.; Fung, J.; Komarnitsky, S.; Siegel, C.; Chuang, W.; Hutto, E.; Shayman, J.; Grabowski, G.; Aerts, J.; Cheng, S.; Copeland, D.; Marshall, J. *Mol. Genet. Metab.* **2007**, *91*, 259.
15. Sugano, H.; Miyoshi, M. *J. Org. Chem* **1976**, *41*, 2352.
16. (a) Xu, J. *Tetrahedron: Asymmetry* **2002**, *13*, 1129; (b) Giles, P.; Rogers-Evans, M.; Soukup, M.; Knight, J. *Org. Process Res. Dev.* **2003**, *7*, 22.
17. Lee, T.; Jones, B. *Terahedron* **1995**, *51*, 7331.
18. For an example of this transformation using AcCl in MeOH, see Nudelman, A.; Bechor, Y.; Falb, E.; Fischer, B.; Wexler, B.; Nudelman, A. *Synthetic Commun.* **1998**, *28*, 471.
19. A549 cells were incubated in the presence of compounds for 72 h. The cells were then stained with fluorescent cholera toxin subunit B (FL-CTB) that binds to ganglioside GM1 on the cell membrane. After fixing the cells with formaldehyde and Hoechst stain, they were analyzed using an automated fluorescent microscope to quantify the amount of GM1 remaining on the cell membrane.
20. Compounds were incubated for 45 min with human liver microsomes (0.25 mg/mL) in the presence of NADPH (1 mmol) and testosterone (20 μM). Substrate conversion was monitored by MS.
21. Compounds (15 μM) were incubated for 30 min with mouse liver microsomes (0.5 mg/mL). Compound depletion was monitored by MS.
22. Biochemical and cell data reported here were obtained in-house according to the text and note 19. The compounds tested were prepared at Exelixis or partner CRO.